THE LOW ENERGY CHARGED PARTICLE (LECP) EXPERIMENT ON THE VOYAGER SPACECRAFT

S. M. KRIMIGIS

The Johns Hopkins University, Applied Physics Laboratory, Laurel, Md 20810, U.S.A.

T. P. ARMSTRONG

Department of Physics, University of Kansas, Lawrence, Kansas 66044, U.S.A.

W. I. AXFORD

Max-Planck Institute for Aeronomy, D-3411 Katlenburg-Lindau 3, West Germany

C. O. BOSTROM

The Johns Hopkins University, Applied Physics Laboratory, Laurel, Md 20810, U.S.A.

C. Y. FAN

Department of Physics, University of Arizona, Tucson, Arizona 85721, U.S.A.

G. GLOECKLER

Department of Physics & Astronomy, University of Maryland, College Park, Md 20742, U.S.A.

and

L. J. LANZEROTTI

Bell Laboratories, Murray Hill, New Jersey 07904, U.S.A.

Abstract. The Low Energy Charged Particle (LECP) experiment on the Voyager spacecraft is designed to provide comprehensive measurements of energetic particles in the Jovian, Saturnian, Uranian and interplanetary environments. These measurements will be used in establishing the morphology of the magnetospheres of Saturn and Uranus, including bow shock, magnetosheath, magnetotail, trapped radiation, and satellite-energetic particle interactions. The experiment consists of two subsystems, the Low Energy Magnetospheric Particle Analyzer (LEMPA) whose design is optimized for magnetospheric measurements, and the Low Energy Particle Telescope (LEPT) whose design is optimized for measurements in the distant magnetosphere and the interplanetary medium. The LEMPA covers the energy range from ~ 10 keV to >11 MeV for electrons and from ~ 15 keV to $\geqslant 150$ MeV for protons and heavier ions. The dynamic range is ~ 0.1 to $\geqslant 10^{11}$ cm^{-2} sec^{-1} sr^{-1} overall, and extends to 10^{13} cm^{-2} sec^{-1} sr^{-1} in a current mode operation for some of the sensors. The LEPT covers the range $\sim 0.05 \leqslant E \leqslant 40$ MeV/nucleon with good energy and species resolution, including separation of isotopes over a smaller energy range. Multi-dE/dx measurements extend the energy and species coverage to 300–500 MeV/nucleon but with reduced energy and species resolution. The LEPT employs a set of solid state detectors ranging in thickness from 2 to ~ 2450 μ, and an arrangement of eight rectangular solid state detectors in an anticoincidence cup. Both subsystems are mounted on a stepping platform which rotates through eight angular sectors with rates ranging from 1 revolution per 48 min to 1 revolution per 48 sec. A 'dome' arrangement mounted on LEMPA allows acquisition of angular distribution data in the third dimension at low energies. The data system contains sixty-two 24-bit scalers accepting data from 88 separate channels with near 100% duty cycle, a redundant 256-channel pulse height analyzer (PHA), a priority system for selecting unique LEPT events for PHA analysis, a command and control system, and a fully redundant interface with the spacecraft. Other unique features of the LECP include logarithmic amplifiers, particle identifiers, fast (~ 15 ns FWHM) pulse circuitry for some subsystems, inflight electronic and source calibration and several possible data modes.

1. Introduction

According to the best available estimates the solar wind extends as a supersonic flow to a heliocentric distance of the order of 50 AU or more, i.e., beyond the orbits of Neptune and Pluto (Axford, 1972). Thus the solar wind must interact with the magnetospheres of all the planets or with their atmospheres or surfaces in cases where the planets have no internal magnetic field. Furthermore, the solar wind must interact with the satellites of any planets which are not shielded by planetary magnetospheres.

The study of the physics of planetary magnetospheres is of considerable scientific interest in itself (Kennel, 1973). It is also of great importance in furthering our understanding of certain astronomical objects (notably pulsars and compact X-ray sources), the origin of satellites of the outer planets, and perhaps the origin of the Solar System itself (e.g., Cameron, 1973; Alfvén and Arrhenius, 1976). The existence of planetary magnetospheres presents opportunities for making direct *in-situ* observations of particle acceleration mechanisms, thereby leading to the possibility of achieving a better understanding of solar flare processes, cosmic ray acceleration processes, and processes in the Earth's magnetosphere. In the case of the Jovian satellite Io (and possibly other planetary satellites) there is an apparent strong interaction with the magnetosphere of the parent planet which induces intense radio emissions by mechanisms which although not well understood at present, could be of importance for understanding other astrophysical radio sources. In addition there is some evidence that planetary magnetospheres can play an important role in determining the surface structure of satellites (Mendis and Axford, 1974).

To date spacecraft launched from Earth have probed the environment around five of the nine planets in the Solar System. Spacecraft instrumentation has also investigated various aspects of the satellites of Earth, Mars and Jupiter. The nature of the Earth's magnetosphere has been investigated in considerable detail and a rather good morphological understanding of the phenomena that can occur has been obtained. Yet, understanding in depth of many detailed plasma processes remains elusive (Williams, 1975). The interaction of the solar wind with the Earth's moon has been investigated extensively; this interaction is a clear case of the impinging of the solar wind plasma on an essentially non-conducting and non-magnetized body that does not have an atmosphere. The bow shock and magnetic tail of the Mercurian magnetosphere have been detected and it has been observed that electron acceleration seems to occur even in this relatively simple case where there are no complications induced by the presence of a planetary atmosphere or ionosphere (Ness *et al.*, 1975). The magnetosphere situations around both Mars and Venus are somewhat unclear at the present time: there appear to be bow shocks and plasma tails associated with each planet and there is also some evidence for a Martian magnetic field of internal origin (Dolginov *et al.*, 1972).

Of the giant planets, the Jovian magnetosphere has been examined during flybys of Pioneer 10 and 11. It is now well documented that for this planet (a) there are

pronounced magnetic field effects associated with the rotation of the planet (Smith *et al.*, 1974); (b) relativistic electrons are present with unexpectedly high fluxes (Fillius and McIlwain, 1974); (c) the Galilean satellites play a significant role in absorbing and perhaps accelerating particles (Fillius and McIlwain, 1974); and (d) energetic particles are injected by the planet into the interplanetary medium (Chenette *et al.*, 1974) where they can be detected even at the orbit of the Earth (Krimigis *et al.*, 1975b). No spacecraft has visited Saturn as yet, but radio emissions from this planet have now been observed (Brown, 1975) so that a Saturnian magnetosphere undoubtedly exists. A unique characteristic of that magnetosphere will be the interaction of energetic particles with Saturn's rings and composition changes or 'sputtering' therefrom.

The planet Uranus will undoubtedly present an essentially new kind of magnetosphere that may well demonstrate some remarkable features. The spin axis of the planet lies essentially in the ecliptic plane and at the time of the expected Voyager encounter in 1986 the axis of rotation of the planet will be pointing at the Sun to within a few degrees (Alexander, 1965). If the axis of rotation and the axis of the dipole component of the magnetic field are roughly coincident (as for the Earth and Jupiter), then the spacecraft will encounter, pole-onward, a rapidly rotating magnetosphere which is lying on its side (e.g., Siscoe, 1975).

The flyby encounters with Jupiter, Saturn and possibly Uranus, although of paramount importance in the design considerations for the LECP, will account for only a few percent of the total time duration of the Voyager mission. Prior to the Jovian encounter, between the Jovian and the Saturnian encounters, and after the Saturnian encounter there exists the opportunity to explore in depth the interplanetary medium at great distances from the Sun. Furthermore, since the two Voyager spacecraft will be in the same region of the Solar System, there will be a unique opportunity for making important correlated measurements among two spacecraft with identical instrumentation in the most distant parts of the heliosphere. Finally, the Voyager spacecraft will be travelling away from the Sun in the general direction of the postulated solar apex.

From the point of view of charged particle observations the Voyager mission and the LECP will make it possible to measure the energy spectra and composition of galactic cosmic rays in a region of space where the effects of solar modulation can be expected to be substantially less than those ever probed previously. The most important interplanetary energetic particle measurements made by LECP will be those investigating: (1) the spectra of the various atomic species comprising the galactic cosmic radiation, especially at low energies; (2) time variations of galactic cosmic rays (including Forbush decreases); (3) the radial gradient of galactic cosmic rays; (4) energetic particles of solar origin associated with flares and active regions; (5) energetic particles of planetary origin such as those observed to be associated with Jupiter as well as the Earth (Krimigis *et al.*, 1975a); and (6) energetic particles associated with interplanetary forward-reverse shock pairs (Smith and Wolfe, 1976). In addition to providing detailed energy spectra, the detector system will make highly

accurate measurements of the anisotropies of low energy cosmic rays and other energetic particles, since such anisotropies can provide a means of identifying the origins of the particles as well as shedding further light on the physics of interplanetary propagation processes.

The LECP contains detector configurations specifically designed to cover the energy range $15 \text{ keV} \leqslant E \leqslant 40 \text{ MeV/nucleon}$ with good energy, angular, and temporal resolution; coverage is also obtained to higher nucleon energies (~300–500 MeV/nucleon), but with lesser energy and species resolution overall.

This system will ideally complement an experiment designed to observe low energy ($\leqslant 10 \text{ keV}$) solar wind and magnetospheric plasmas, a magnetometer experiment, appropriate wave experiments, and a cosmic ray instrument at much higher energies. Fortunately, all of these experiments are included in the comprehensive Voyager payload.

2. Scientific Objectives and Background

The Voyager mission represents a unique opportunity to perform exploratory measurements at Saturn and probably Uranus, in the outer extremes of the interplanetary medium and (possibly) in the interstellar medium, and to conduct 'second generation' studies of the Jovian environment. The LECP instrument is designed to address the following objectives:

(1) Investigate the existence, spatial extent and dynamical morphology of Saturnian and Uranian magnetospheres and measure the spectral and angular distributions, composition and plasma flows of particles in the radiation belts, bow shock, transition region and magnetotail; determine the planetary and satellite magnetic moments and the nature of nonthermal radio emission.

(2) Investigate the quasi-steady energetic particle flux in interplanetary space for studying solar modulation mechanisms, the radial gradient and radial scale of modulation, short term modulation effects, the solar, galactic, and planetary components, and particle acceleration mechanisms in the interplanetary medium, and (possibly) the terminus of the heliosphere.

(3) Perform 'second generation' studies of the composition, energy spectrum, azimuthal and pitch angle distribution of Jovian magnetospheric charged particles bearing on questions of origin, transport, loss, and of sources of decameter and decimeter radio emission, including important satellite sweeping and source effects.

(4) Study the energetic particle environments of natural planetary satellites and deduce satellite magnetic moments, conductivities, and the electrodynamics of the interaction with the planetary magnetospheres (e.g., particle 'shadowing' studies and searches for field aligned particle currents).

(5) Make inferences concerning the origin and interstellar propagation of galactic cosmic rays, their confinement times and path length distributions, by measuring the elemental and isotopic composition and anisotropy of galactic particles after the Saturnian (Uranian) encounter.

(6) Study the propagation in the distant interplanetary medium of particles emitted at the Sun by investigating their intensity-time profiles, energy spectra, gradients, and anisotropies and the charge and isotope composition.

(7) Investigate large and small scale magnetic structures in the interplanetary medium and near planets using charged particle angular distributions in order to augment magnetometer measurements.

Because of space limitations, it is not possible to give an adequate discussion of the science background for all the objectives enumerated above. Thus we will limit our remarks to a few specific points which are illustrative of the measurement and interpretive possibilities utilizing the LECP data.

A. PLANETARY MAGNETOSPHERES

The first and most important objective here is the establishment of the morphology of the magnetospheres of Saturn and Uranus. Aside from this general objective, however, our experiment is especially designed to address specific problems within the magnetospheres of both planets, and of Jupiter as well. First we expect to obtain the three-dimensional distribution function of low energy electrons and ions, which is an essential tool in the study of wave-particle interactions and the underlying physical processes which give rise to plasma instabilities in planetary magneto-spheres (e.g., Williams and Lyons, 1974). In addition we will obtain the composi-tional signature of energetic ions and thus be able to infer their sources, i.e., whether these ions originate in the solar wind, planetary ionosphere, or are 'sputtered' off planetary satellites, as appears to be the case at the orbit of Io (Brown, 1973). Further, the experiment is designed to make detailed angular distribution measure-ments while the spacecraft is traversing the Io flux tube at a distance of ~10 satellite radii. During this passage, the importance of Io as both a source and sink of energetic particles will be determined in a rather comprehensive manner. The implications of this measurement on the Io-associated decametric radio emissions is evident.

In addition to the above measurements, the low energy (~15 keV) proton threshold on the LEMPA allows direct measurement of moving hot plasmas of sufficiently high density. We have reported plasma flow and temperature measure-ments in the Earth's magnetotail, magnetosheath and upstream bow shock region (Roelof *et al.*, 1976) using a detector with somewhat higher energy threshold (50 keV) and a geometric factor of only $\sim\frac{1}{4}$ that of the LEMPA. Our technique deduces both the plasma bulk velocity and temperature from the anisotropy of the sectored fluxes. The sensitivity of the LEMPA to a moving Maxwellian plasma is illustrated in Figure 1. The peak integral flux from the direction of the plasma flow divided by the density (J_0/N) is given as a function of 'thermal energy' $E_{th} = kT$ in Figure 1a for $\geqslant 15$ keV protons for three bulk flow velocities (and for $\geqslant 10$ keV electrons, which are insensitive to plasma flow). The sample angular distribution (given in Figure 1b) for a 1 keV plasma flowing at a relatively low velocity of 100 km s^{-1} exhibits an anisotropy sufficiently strong to determine the proton tem-perature. At a moderate 300 km s^{-1} (typical of the terrestrial magnetosheath), a

plasma of density $10^{-2}\,\mathrm{cm}^{-3}$ would yield $\sim 10^2$ counts in the peak sector of the $\geqslant 15\,\mathrm{keV}$ proton LEMPA channel (while rotating at 1 RPM), allowing $\sim 10\%$ statistics for an anisotropy 'snapshot' every minute. In addition, Figure 1a demonstrates the high sensitivity of the $\geqslant 10\,\mathrm{keV}$ electron LEMPA channel to hot plasma (independent of bulk velocity), with rates $\sim 10^2\,\mathrm{s}^{-1}$ even for densities as low as $10^{-6}\,\mathrm{cm}^{-3}$. Thus the lowest energy LEMPA channels are capable of measuring the
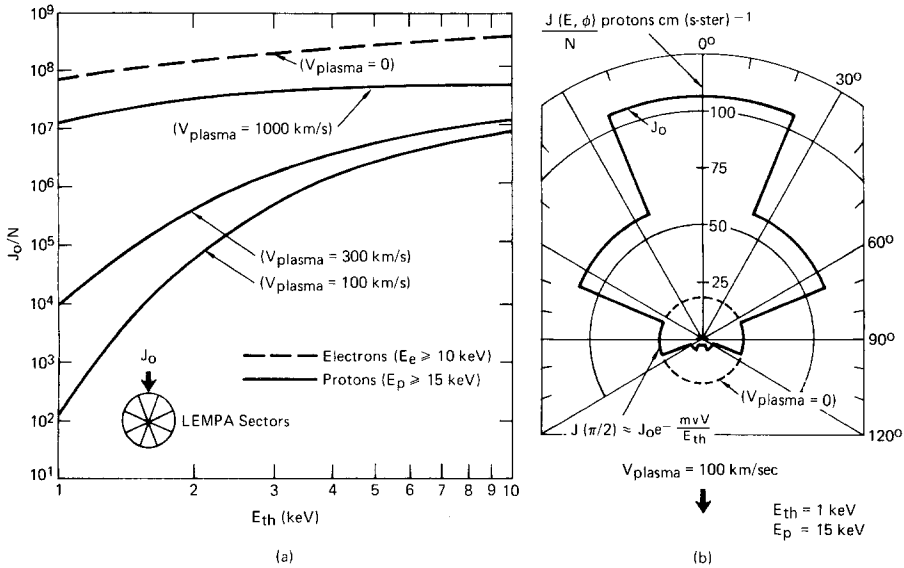

Fig. 1.   (a) Integral flux in peak LEMPA sector (direction of plasma flow divided by plasma density J_0/N) for energy thresholds $E_p \geqslant 15\,\mathrm{keV}$ (for three flow velocities) and $E_e \geqslant 10\,\mathrm{keV}$ (negligible dependence on flow velocity) as a function of plasma temperature ($E_{\mathrm{th}} = kT$).
  (b) Angular flux distribution (integral above $E_p = 15\,\mathrm{keV}$ plasma flowing at $100\,\mathrm{km\ s}^{-1}$). (Courtesy of Drs E. C. Roelof and R. E. Gold.)

high energy tail of plasmas with $kT \geqslant 1\,\mathrm{keV}$, while the higher energy channels span the physically important transition region to the nonthermal energy region ($\sim 300\,\mathrm{keV}$) that often accompanies hot plasma flow as is the case in the outer terrestrial magnetosphere (Sarris *et al.*, 1976). Measurements of such plasma flows have proved to be essential in delineating the dynamics of the Earth's magnetotail, including the substorm process and the 'plasma mantle' (Rosenbauer *et al.*, 1975).

B. ENERGETIC PARTICLE MEASUREMENTS IN THE INTERPLANETARY MEDIUM

The recent reports of observations of solar particle events with long-lasting anisotropies, together with the measurements of very small cosmic ray radial gradients by Pioneer 10 and 11 instruments have raised several interesting and important questions about the underlying theoretical considerations of both the modulation and energy loss of galactic cosmic rays in the Solar System as well as of the size of the solar modulation region. In addition, the important recent discoveries of planetary

particle contributions to the interplanetary particle fluxes (Teegarden et al., 1974; Chenette et al., 1974; Krimigis et al., 1975a) and the anomalous abundance of low energy C and O nuclei (Klecker et al., 1975) reveal a situation considerably more complex than the hypothesis that all low energy cosmic rays observed near 1 AU result from the energy losses of low energy galactic particles entering the solar modulation region (Fisk et al., 1974).

The degree of our understanding of cosmic-ray propagation in the heliosphere can be measured by the consistency of our explanation of particles streaming (a) from the Sun (b) from planetary magnetospheres and (c) from the galaxy. The persistent anisotropies of solar flare particles of energies $1-10^3$ MeV (Roelof and Krimigis, 1973; Innanen and Van Allen, 1973; Duggal and Pomerantz, 1973; Wibberenz et al., 1976), the very small values of the radial cosmic-ray gradients out to 5 AU (Thomsen and Van Allen, 1976) and the appearance of Jovian magnetospheric particles near Earth (Krimigis et al., 1975b) all seem to indicate that the region of the Solar System within ~5 AU is characterized by relatively weak scattering of cosmic rays. If so, then the control of the 11-year solar modulation of cosmic ray intensity must lie in the region beyond 5 AU (unless the modulation and scattering mechanism is not at all adequately understood). Because of the possibly large extent of the modulation region (Axford, 1972) and because the cosmic ray radial gradient at any given energy is unlikely to be uniform as a function of heliocentric distance, our instruments on the two Voyager spacecraft will allow gradient measurements at points separated by relatively short distances (i.e., a few AU), as well as between instruments at large heliocentric distances and at the orbit of Earth.

C. SOLAR AND PLANETARY PARTICLES AS PROBES OF THE INTERPLANETARY MEDIUM

Solar energetic particle events provide valuable diagnostics of the large and small scale interplanetary plasma and magnetic field at large heliocentric distances. The sensitivity of a traditional tool used for solar event analyses, i.e., study of the velocity dispersion of event onsets, increases approximately as the square of the heliocentric radius for field-aligned propagation. Hence the persistence at large heliocentric distances of an anti-sunward field-aligned anisotropy as well as the development of a 'back-scattered' flux in the sunward direction will provide important diagnostics (even more sensitive than at 1 AU) on small scale magnetic irregularity structures inside and outside (respectively) the orbit of the spacecraft. The ability of the LECP to cleanly separate atomic species and isotopes during solar events will allow an analysis of Z/A propagation effects in the outer solar system.

In addition, both the Earth and Jupiter are sources (albeit of widely differing strengths) of low energy interplanetary particles with spectral, temporal and abundance signatures distinguishable from solar events. Consequently, planetary magnetospheres can also provide particles as 'tracers' of the large scale interplanetary field, at large distances, both upstream and down stream of the planet. LECP will provide the necessary energy, abundance, and anisotropy data to make strong use of these tracers.

Finally, interplanetary acceleration of energetic particles has been observed to occur both at 1 AU and in the outer Solar System. Three main mechanisms have been discussed in the literature with regard to particle acceleration (or deceleration) in the interplanetary medium; shock-associated acceleration (essentially in the shock electric field); adiabatic deceleration (essentially a gas-dynamic cooling due to expansion); and *in-situ* acceleration (supposedly a second-order Fermi process).

A critical evaluation of the two basic classes of particle shock-acceleration models (microscopic plasma dynamics and post-shock magnetic field) will be possible using our LECP anisotropy and spectral measurements of electrons and ions since the post-shock regions in the outer solar system will often differ substantially from those at 1 AU. The composition dependence of the shock effects (e.g., Armstrong and Krimigis, 1973) is of great interest under the shock conditions at large heliocentric distances.

Adiabatic deceleration occurs when particles are effectively 'convected' by the solar wind due to efficient scattering. Our LECP anisotropy and energy spectrum data will permit us to evaluate the possible importance of this process in the outer solar system.

3. Description of Instrumentation

Measurements fulfilling the requirements of the comprehensive investigation objectives described in the previous sections cannot be conducted with a single charged particle sensor. To attain the lowest energy of response over a wide variety of particle species and with appropriate geometry factors and angular resolution, the LECP utilizes two distinct all solid-state detector configurations each of which is optimized for a particular energy-intensity range and/or group of particle species. This procedure has the additional important advantage of providing overall experimental redundancy. The two detector subsystems designated as (a) The Low Energy Magnetospheric Particle Analyzer (LEMPA) and (b) The Low Energy Particle Telescope (LEPT) are described in the next two subsections. A picture of the flight instrument is shown in Figure 2. Both of these detector subsystems use multi-parameter detection techniques to provide measurements in overlapping energy and intensity ranges; this redundancy increases system reliability and reduces background. Although the individual subsystems are optimized for either the interplanetary or magnetospheric environments, both subsystems will contribute substantial measurements which are important to both environments (Figure 8). The sunshield used for both subsystems provides an additional unique and important function in that we are able to unambiguously determine the background counting rates for all system detectors and channels in both environments. Also, small radioactive sources for inflight calibration are mounted on the sunshield. Since the detector design was done prior to the Pioneer 10 encounter of Jupiter, certain changes were necessitated following the publication of the Pioneer results. The most important of these changes was the addition of substantial shielding to appropriate detector subsystems.
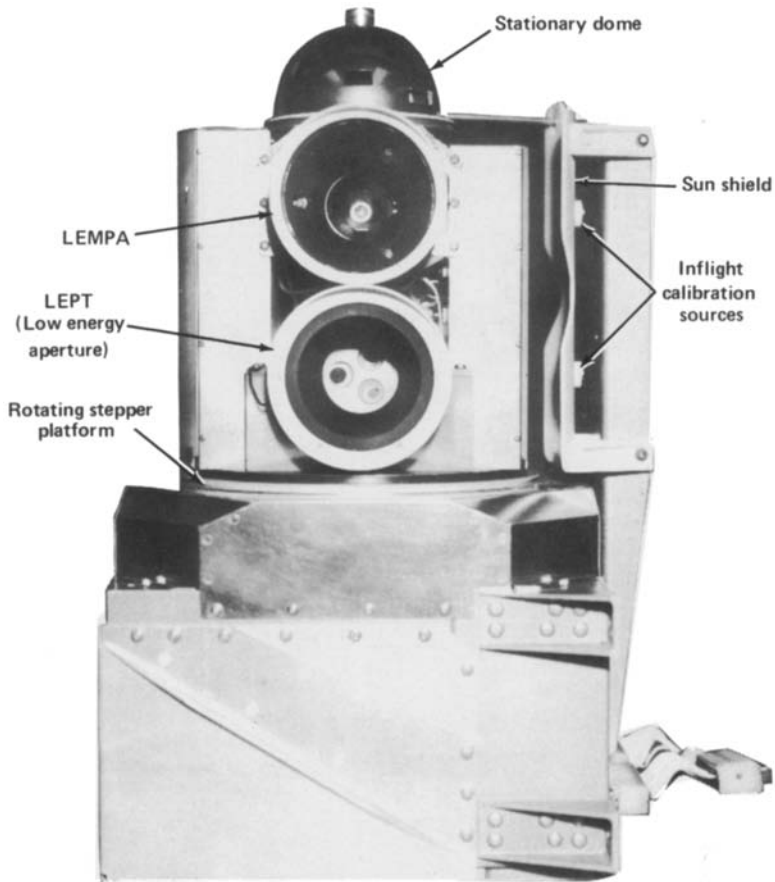
Fig. 2. A picture of the first flight unit of the LECP experiment. The low energy aperture of both LEMPA and LEPT are shown; the high energy apertures are facing in the opposite direction (180°). Inflight radioactive calibration sources are mounted on the sun shield for both LEMPA and the LEPT. The entire assembly (including two electronics boxes) above the stepping platform is rotated into eight angular sectors.

A. LOW ENERGY MAGNETOSPHERIC PARTICLE ANALYZER (LEMPA) SUBSYSTEM

The detectors in the LEMPA subsystem are designed for low energy thresholds (10–15 keV), clean separation of ions from electrons, good sensitivity, and large ($\sim 10^{11}$) dynamic range.

A schematic diagram of the detector arrangement in the LEMPA subsystem is shown in Figure 3. The functions of each detector are as follows:

Detector α (protons, ions)

This is the primary detector for measuring protons-ions at low energies ($\geqslant 15$ keV) with high sensitivity ($G \sim 0.12$ cm^2 sr) and good energy resolution. It consists of a
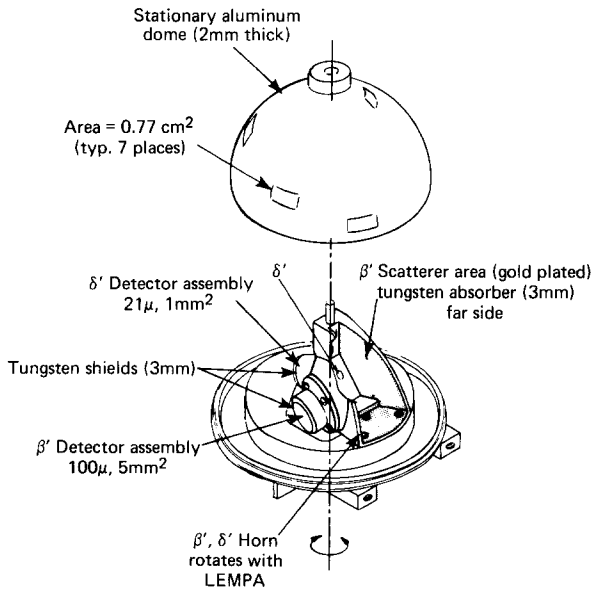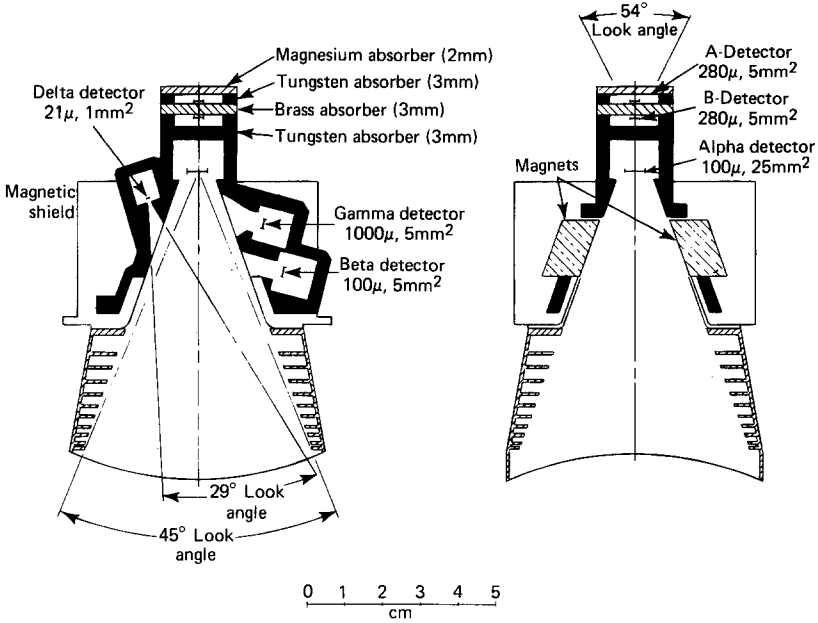
Fig. 3.   Schematic drawing of the LEMPA and dome detector assembly. Incoming electrons are swept away from detector α by the magnet and counted in detectors β and γ. Detectors δ, δ' are insensitive to electrons of any energy. Tungsten shielding eliminates interference from high energy penetrating electrons in most parts of the Jovian magnetosphere. Thicknesses for detectors are nominal.

25 mm^2, 100 micron surface barrier totally-depleted detector, with the aluminum side facing the incoming particle flux (to minimize radiation damage). A rare-earth alloy magnet is used to deflect electrons with energies $\leqslant$400 keV away from the detector. These electrons are subsequently counted by detectors β and γ as described in the next paragraph. The output from the α detector is fed into window-type discriminators which provide information in 10 proton-ion differential channels at all times. The energy channels cover the range $\sim$0.015 to 4 MeV for protons and ions and 4 to 16 MeV for alphas. The actual energy passbands, based on calibrations of the first flight unit, are shown in Figure 4a. A gain switch has been included in the Pα1 channel so that the lowest threshold can be increased to $\sim$25 keV, should the system noise increase for any reason. The background counting rate of this detector due to the presence of the spacecraft RTG is expected to range from 3×10^{-2} to 4.5×10^{-3} c/sec, i.e., at least an order of magnitude below the omnidirectional cosmic ray background. Note that tungsten shielding equivalent to the range of $\sim$15 MeV electrons minimizes background for most of the anticipated flyby trajectory at Jupiter.

Detector β and γ (electrons)

These detectors are the primary ones for the measurement of low energy ($\geqslant$15 keV) electrons over a wide dynamic range with good sensitivity ($G \sim 0.002$). Detector β is 5 mm^2, 100 μ thick, while detector γ is 5 mm^2, 1000 μ thick; they are designed to measure the low and intermediate energy portions of the electron spectrum, respectively. The incoming beam of electrons is bent by the magnet onto the detectors for pulse height analysis and intensity measurements. The geometric factors and fields of view of detectors β and γ have been evaluated both by trajectory-tracing of electrons of various energies in actual magnetic field geometries and by initial calibration of the Voyager prototype experiment. The angular response for monoenergetic beams of electrons for the first flight unit is shown in Figure 4b, and it is evident that 10 keV electrons are readily counted by detector β. The differential channels at maximum response are shown in Figure 4c. Both detectors are designed to measure large fluxes in the Jovian magnetosphere and at the same time be capable of measuring interplanetary electrons such as those emitted in solar particle events. The energy spectra available from detector β during planetary encounter will be crucial in examining, in depth, particle acceleration and loss processes associated with satellite interactions in the planetary magnetospheres. Both of these detectors are also shielded from electrons with $E \leqslant 15$ MeV. This shielding, however, may not be sufficient to prevent background contamination at closest approach ($L \sim 5R_J$) if the electron energy spectrum is indeed flat below $\sim$160 keV (Fillius and McIlwain, 1974).

Detector β' (electrons)

This detector is used to measure electrons over the same energy intervals as detector β (10 to 200 keV) but with a field of view centered 90° from that of β and

perpendicular to the ecliptic plane (Figure 3). Its main function is to provide detailed angular distribution measurements not only in planetary magnetospheres, but also in the interplanetary medium. Essentially complete electron pitch angle distributions are obtained during magnetospheric encounters by the use of the umbrella-like passive shield with narrow rectangular look angles. The dome is mounted on a shaft coincident with the axis perpendicular to the ecliptic plane about which the stepping
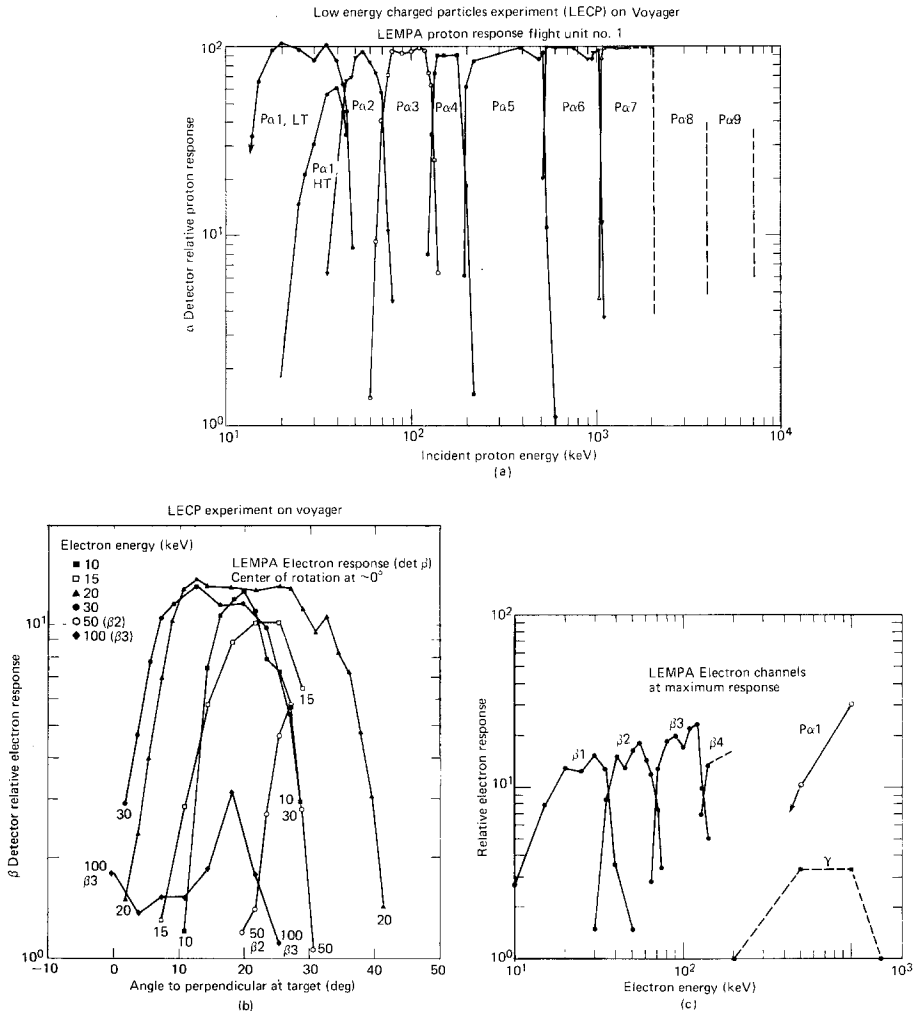

Fig. 4.   (a) Experimental response of detector α in LEMPA to protons; LT and HT denote 'low threshold' and 'high threshold', respectively in channel Pα1. Dashed lines indicate expected thresholds at high energies.

(b) Angular response of detector β in LEMPA to a undirectional beam of incident electrons; note that 10 keV electrons are readily counted by the detector.

(c) Data from the same calibration as in (b), but showing the differential energy channels at maximum electron response. Preliminary data for detectors γ and α are also shown.

motor (see below) rotates the LEMPA and LEPT subsystems. Detector β' is a 5 mm^2, 100 μ thick solid state sensor located in a scatter geometry from the field of view (Figure 3). Electrons are single-scattered by more than 90° from a gold foil and are incident on the detector where they are pulse-height analyzed in 5 energy channels. The electrons scatter efficiently ($\sim$1–10%) over most of this energy range resulting in an efficiency-geometric factor of $\sim$0.002 cm^2 sr^{-1}. Protons arriving through the open aperture cannot reach the detector, although high energy ($>$70 MeV) protons can penetrate the aluminum dome and the detector shield and contribute to the counting rate. The shielding thickness has been determined after review of the Pioneer 10 and 11 results. The RTG background is identical to that for detector β and does not interfere with the proposed measurement objectives.

Detector δ (High Intensity Protons, α's and $Z \geqslant 3$ Nuclei)

The purpose of detector δ is to obtain high intensity proton, alpha particle and $Z \geqslant 3$ nuclei composition, energy spectra, and three-dimensional angular distributions in the Saturnian, Uranian and Jovian radiation belts. The design is optimized for a radius of closest approach of $\sim$5R_J and for the proton environment measured by Pioneers 10 and 11. The sensor consists of a $\sim$20 μ, 1 mm^2 totally-depleted surface barrier solid state detector of the type repeatedly flown in the Earth's radiation belt over the past several years. The output from this detector is fed into a fast ($\sim$15 ns FWHM) charge-sensitive pre-amplifier followed by several threshold discriminators which provide proton, alpha particle, and $Z \geqslant 3$ measurements over the range $0.25 \leqslant E \leqslant 2$ MeV/nucleon. The maximum apparent counting rate of this detector is $\sim$4 $\times$ 10^6 c/sec while the true counting rate corresponds to $\sim$10^8 c/sec. With a geometric factor of $\sim$10^{-3} cm^2 sr^{-1}, the maximum measurable flux is $\sim$10^{11} cm^{-2} sec^{-1} sr^{-1}, i.e., well above the anticipated Jovian environment at $L \simeq$ 5R_J.

Detector δ' (Protons, ions)

This detector is used to measure protons and ions at the same energy intervals as detector δ but with a field of view ranging up to 90° away from that of δ by sharing the umbrella passive shield with detector β' (Figure 3). Together, detectors δ and δ' provide essentially complete three-dimensional proton and ion pitch angle distributions during magnetospheric encounters. Detector δ' is a 1 mm^2, 20 μ thick solid state detector and utilizes the same electronics as detector δ.

Detectors AB (High Intensity – High Energy)

Detectors AB are included in the LEMPA package to increase the dynamic range of the system in both energy and intensity to values well above those measured by detectors α, β, and γ. Both devices are 5 mm^2, $\sim$300 μ thick surface barrier detectors spaced $\sim$5 mm apart inside shielding material. In the forward direction detector B is shielded by 2.6 g cm^{-2} brass and detector A by 0.35 g cm^{-2} magnesium. The detectors are operated in both a coincidence and a singles count-rate mode. The

outputs from each detector are fed into fast (~50 ns FWHM pulse) charge-sensitive preamplifiers followed by the appropriate discriminator and logic circuitry. This circuitry, together with the shielding configurations, define two semidirectional (i.e., responding mostly over the forward 54°) electron channels in the range ~1.3–20 MeV, one coincidence directional electron channel >11 MeV, and two semi-directional proton channels in the range 15–150 MeV. In addition, single detector counting rates are monitored corresponding to differential proton channels and single electron channels with maximum apparent rates of ~20×10^6 c sec^{-1} corresponding to true rates of ~10^9 c sec^{-1}. The omnidirectional geometric factor for each detector is 3×10^{-2} cm^2 while the directional AB factor is 10^{-2} cm^2 sr^{-1}. Hence, it is possible to obtain directional intensities of high energy electrons with fluxes up to at least 10^9 cm^{-2} sec^{-1} sr^{-1}, while singles rates due to protons and electrons together can be used to measure omnidirectional particle fluxes >10^{11} cm^{-2} sec^{-1}. The capability of this detector configuration exceeds the intensity values measured at the planned Voyager distance of closest approach to Jupiter. For an exploratory mission to Saturn and Uranus, however, such a capability is an absolute necessity.

Current Mode Operation

Although the LEMPA subsystem can handle particle intensities up to 10^{11} cm^{-2} sec^{-1} sr^{-1} in a discrete particle counting mode (entirely adequate for the Jovian encounter), there exists the possibility that higher fluxes of low energy (<1 MeV) particles may be encountered in the Saturnian and Uranian radiation environment. To prepare for such an eventuality a current mode operation has been included for LEMPA sensors α and β thereby extending the dynamic range to fluxes ~10^{13} cm^{-2} sec^{-1} sr^{-1}. In this mode the current due to the energy loss of incoming particles from each detector is monitored over the range 5 nanoamperes to 5 microamperes.

B. LOW ENERGY CHARGED PARTICLE TELESCOPE (LEPT) SUBSYSTEM

The LEPT subsystem is an array of solid state detectors designed to measure the charge and energy distributions of low and medium energy nuclei in environments where the intensity is expected to be relatively low (e.g., outer regions of planetary magnetospheres and the interplanetary and (possibly) interstellar mediums). The detector arrangement is shown schematically in Figure 5, and consists of two multi-dE/d$x \times E$ systems placed back to back in order to use a common all solid-state active anticoincidence shield.

Particular emphasis has been placed on achieving the lowest energy of response attainable with solid state detector telescopes. The proposed configuration will measure the energy of, and separately identify protons and heavier nuclei from ~0.1 to $\geq$40 MeV/nucleon (two or three parameter measurements). One-parameter and multi-dE/dx measurements extend the energy range to ~0.05 and $\geq$500 MeV/nucleon. The specific functions of each detector element are given below.

51° Look angle

D4-Detector 2450μ, 850mm²

D3-Detector 2450μ, 850mm²

D2-Detector 150μ, 800mm²

60° Look angle

Nickel foil 0.7 mg/cm² (2000 A evaporate al overcoat)

D5-Detector 90μ, 800mm²

Anti-coincidence detectors 1500μ typ. 8 places

D1$_A$-Detector 5μ, 50mm²

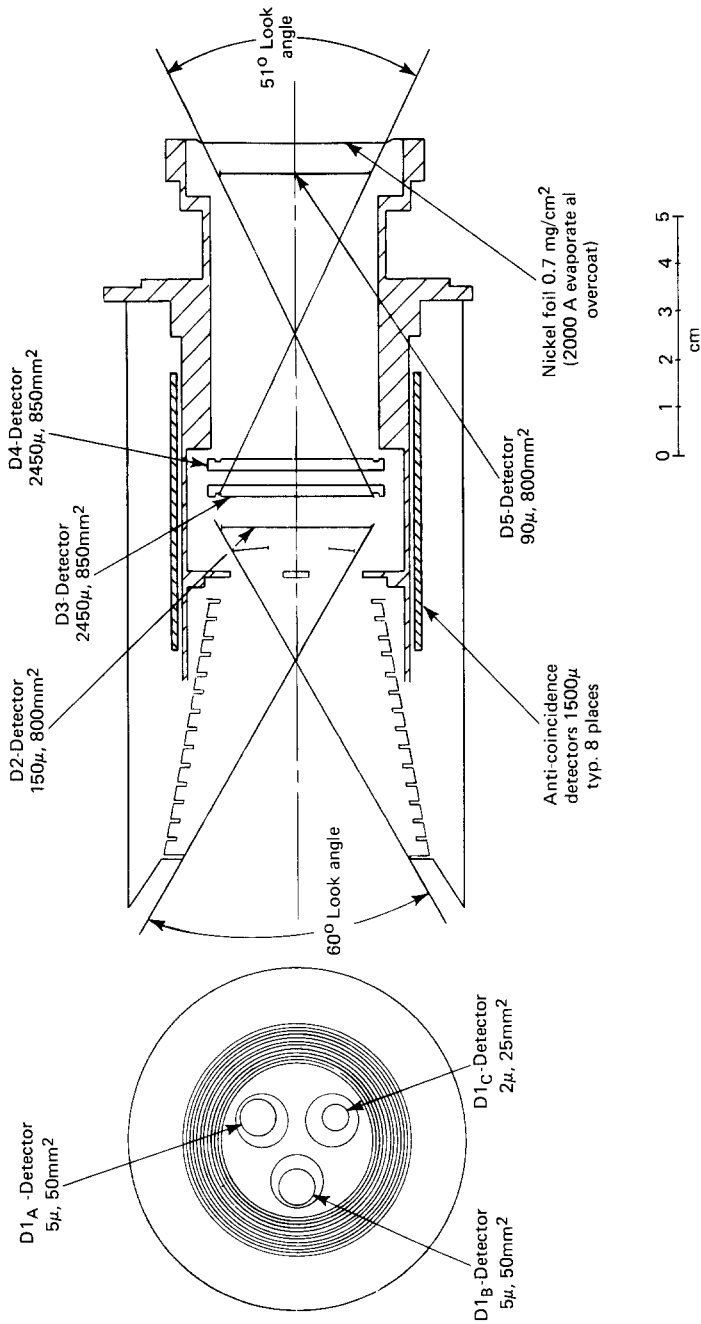D1$_C$-Detector 2μ, 25mm²

D1$_B$-Detector 5μ, 50mm²

cm
0 1 2 3 4 5

Fig. 5. Schematic diagram of the LEPT assembly. Detector thicknesses and areas may differ somewhat between the first and second flight units.

Detector D1

The first detector of the LEPT dE/dx vs E system consists of a set of two ~5 μ thick, 50 mm^2 and one ~2 μ thick 25 mm^2 surface barrier detectors. Each detector is arranged at an appropriate angle to the axis of the telescope so that variation of the ΔE signal over the angular field of view of the telescope is minimized. The signals from each of the units are independently amplified and fed to several window type discriminators (for counting rate information), to a particle identifier system (for species rate and priority data with detector D2), and for sampling by a 256 channel pulse-height analyzer.

Detector D2

This large area (8 cm^2), ~150 μ thick detector serves as the total E detector for LEPT for particles penetrating the D1 detectors. It is operated in anticoincidence with detectors A1 to A8, and in coincidence with detector D1. Pulses from this detector are log-amplified and fed into threshold discriminators for rate data and into a 256 channel pulse-height analyzer. The D1 and D2 signals are used in one of the particle identifier systems to provide good species resolution in a counting mode which greatly increases the dynamic range of the pulse-height analyzer scheme. For example, the identifier system can accept up to ~10^5 events per second while the PHA can only transmit ~1 to 2 events per second. The ΔE vs ΔE signals in the D1, D2 combination are shown in Figure 6a for detectors in the first flight unit of LECP. The error bars are FWHM values and represent the expected energy resolution of the system as verified from prototype calibrations. Solid lines in this figure denote the boundaries of several particle identifier channels with telemetry duty cycles of 100%, as discussed above. Figure 6b shows data from the calibration of the first flight unit at the Rutgers/Bell Tandem Van-de-Graaff accelerator, and includes nuclei of He^3, He^4, Li^6, O^{16}, S^{32}, and Fe^{56}. The curves expected on the bais of Figure 6b have been sketched in. A histogram across the helium lines shows separation of the He^3 and He^4 peaks by 7 channels, although the density of points in Figure 6b makes this isotope separation invisible.

Detectors A1–A8

These detectors define an anticoincidence cylinder and have typical dimensions of 2.3 cm × 6 cm × 1 mm. Such detectors are highly preferable to scintillator-photomultiplier combinations for anticoincidence logic. Each pair of detectors has a separate preamplifier-amplifier chain and can be commanded off separately. By connecting two pairs of detector outputs together, two separate measurements of the omnidirectional penetrating particle rate are obtained. Detectors A1–A4 are fed into a common discriminator as are A5–A8; thus, the coincidence rate between the two (independent) halves of the anticoincidence cup is relatively free of the background induced by the onboard RTG power supply.
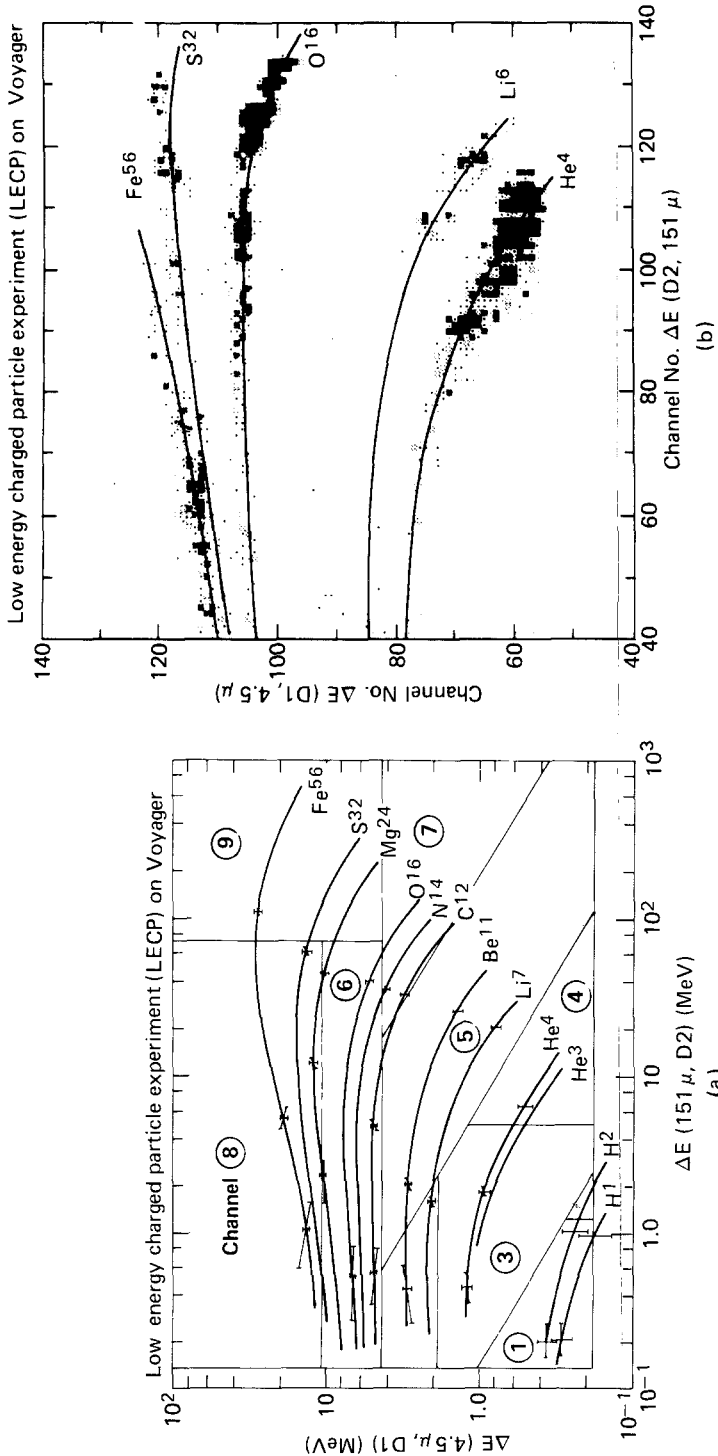
Fig. 6. (a) ΔE vs ΔE plot for the D1a, D2 detectors on flight unit No. 1. Actual detector thicknesses and system noise levels have been used. Thick solid lines show the boundaries of rate channels defined by onboard logic and particle identifier circuitry. Circled numbers indicate the channel number, while energy levels indicated along both axis give the discriminator thresholds for each detector.

(b) Calibrations at the Rutgers/Bell Tandem Van-de-Graaff accelerator with He^3, He^4, Li^6, O^{16}, S^{32} and Fe^{56}

Detectors D3 and D4

These detectors are used in a dE/dx vs E combination to extend the energy range of the telescope from ~4 to ~40 MeV/nucleon. Both detectors are 2450 μ thick, 8.5 cm^2 lithium drifted detectors which serve as total E sensors. The signals from both D3 and D4 are log-amplified and fed into threshold discriminators and pulse-height analyzers, in the same manner as in the case of the D1, D2 and D5 detectors. Both are in anticoincidence with the 8 A detectors, to insure appropriate particle angular response and energy definition as well as to minimize background.

Detector D5

This detector is ~90 μ thick, 8 cm^2 and is used as a ΔE detector in the medium energy end of the LEPT. In combination with detectors D3 and D4, the output of detector D5 is fed to the particle identifier system to provide species rate data and priority information for the detailed pulse height analyses. The expected ΔE signals from the D5, D4 combination are plotted in Figure 7. It is evident from the figure that good isotope resolution is expected from hydrogen on up, including oxygen. Appropriate particle identifier channels are also shown on this diagram.
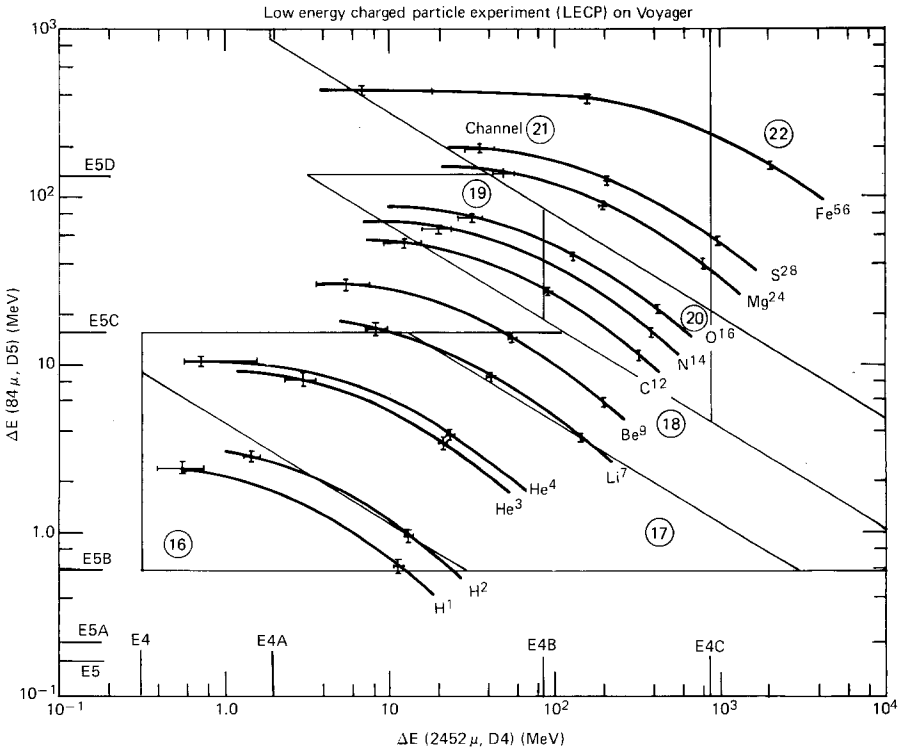

Fig. 7.   Same as Figure 6a but for the D5, D4 detectors in flight unit No. 1. Calibrations have verified the expected response.

Logarithmic Amplifiers and Particle Identifiers

The use of logarithmic amplifiers enables us to employ simple adder circuits in order to calculate the relationship $\Delta E \simeq \alpha E^{\beta}$ for particle energy loss in the silicon detectors. The simple electronic computation of a particle's energy loss in each of a series of detectors makes possible the use of an onboard particle identifier, resulting in greatly improved rate data for major charge groups. Further, the use of the particle identifier information enhances the utility and effectiveness of the priority system. Most importantly the logarithmic amplifiers give constant resolution throughout the entire energy range of response of a detector (from ~0.1 to >1000 MeV).

Priority Scheme

As noted above, it is not possible to transmit more than 1 or 2 pulse-height analyzed events/second due to bit-rate limitations. Incorporated in the system logic is a rotating three-level priority scheme which is based upon particle Z (atomic number). Group I contains channels responding to heavy nuclei and have the highest priority in pulse height analysis; Group II contains channels of light and medium nuclei (second priority), while Group III includes those channels responding to protons and alpha particles (third priority). To insure, however, that all groups are equally represented in environments with relatively intense fluxes of all species, the priority is rotated according to the event read out last. If the last event belonged to Group I then, after readout, Group II has the highest priority and Group III will be intermediate; if the event read out last belonged in Group II, then Group III would have the highest priority and I will be intermediate; finally, if the event read out was in Group III, then Group I will have the highest priority and Group II will be intermediate. In this manner, equal statistical weight will be obtained for all particle species in relatively intense environments. This is particularly important in the distant magnetosphere of Jupiter where large fluxes of low energy ions are expected to be present.

Geometric Factors

The geometric factor for D1D2$\overline{\text{D3}}$ events is ~0.48 cm^2 sr^{-1}, while that for D2D3D4 events is ~2.3 cm^2 sr^{-1} and that for D5D4$\overline{\text{A}}$ events is ~1.7 cm^2 sr^{-1}. For penetrating particles (D3D4$\overline{\text{A}}$) the geometric factor is ~4 cm^2 sr^{-1}. The characteristics of the LEPT system are summarized in Table I. The energy coverage for both the LEPT and LEMPA subsystems is shown in Figure 7.

Stepping Platform

The scientific importance of making anisotropy measurements for both the cruise and encounter phases of the mission was emphasized in Sections I and II. Because the Voyager spacecraft has a fixed orientation, it is not possible to obtain angular distribution measurements in the ecliptic plane by utilizing spacecraft spin. It is therefore necessary to use either multiple detector heads ȯr to rotate the detector system at some appropriate rate. The latter method has been chosen as the most

TABLE I

Summary of detector characteristics-LECP

Detector designation	Detector description	Energy response Nucleons (MeV/nuc) or electrons (e⁻, MeV)	Nuclear charge range[a]	Number of parameters measured	Geometric factor cm² sr	Dynamic range[b] cm⁻² sec⁻¹ sr⁻¹
	Det α Low energy protons & ions	$0.02-4, p$ $1-4, \alpha$	$Z \geqslant 1$ $Z \geqslant 2$	2^c	0.12	$0.3-10^7$ (to $\sim 10^{12}$ in C.M.)
	Det β Low energy electrons	$0.015-0.2, e^-$	—	2	~0.002	$50-10^8$ (to $\sim 10^{13}$ in C.M.)
LEMPA Low energy magnetospheric particle analyzer	*Det γ* Medium energy electrons	$0.2-1, e^-$	—	2	0.002	$10-10^8$
	Det δ, δ' High intensity composition	$\sim 0.26-7, p$ $\sim 0.375->4, \alpha$ $\sim 0.375->12, Z \geqslant 3$	$Z = 1$ $Z = 2$ $Z \geqslant 3$	1^d	0.002	$\sim 0-10^{11}$
	Det AB High energy-high intensity protons and electrons	$15-150, p$ $>1.4, e^-$ $>11, e^-$	$Z \geqslant 1$ —	1 1	0.03	$\sim 0-5 \times 10^{11}$
	Det β' electrons ⊥ to ecliptic	$0.015-0.2, e^-$	—	2^e	0.002	$5-10^8$

Low energy particle aperture	Ultra low energy	0.093–0.18	$Z \geq 2$	1	~0.1	~$0-10^5$
	Total $E(2\mu)$	0.047–0.14	$Z \geq 4$			
	Ultra thin	0.48–1.4	$Z=1$			
	dE/dx vs E	0.15–3.0	$Z=2$	2	~0.5	~$0-10^5$
		~0.13–10[f]	$Z=3-10$			
		~0.07–13	$Z=11-28$			
	Multi	3–31	$Z=1, 2$			
	dE/dx vs E	6.3–60	$Z=3-10$	2, 3	~4.0	~$0-10^5$
		7.4–115	$Z=11-28$			
		>0.5, e^-	—	2		
LEPT Low energy particle telescope	Four parameter	31–220	$Z=1, 2$	4	~2.3	~$0-10^5$
	dE/dx	60–270	$Z=3-10$	4	~2.3	
		115–∞	$Z=11-28$	4	~2.3	
High energy particle aperture	D3D4 High sensitivity penetrating	≥200	$Z=1$	2	~20	~10^6 c/day[g]
		>4, e^-	—	2	~20	
	Anticoincidence	≥20	$Z \geq 1$	1	~28 cm^2	~10^7 c/day[g]

[a] Approximate energy ranges for Isotope Resolution:

$Z=1, 2$	0.2–30 MeV/nucl.	(approx.)	($\Delta M = 1$)
$Z=3-8$	1.0–60 MeV/nucl.	(approx.)	($\Delta M = 1$)
$Z=9-16$	3.0–90 MeV/nucl.	(approx.)	($\Delta M = 2$)

[b] Dynamic ranges are approximate. In current mode (C.M.), charge and energy resolution comments do not apply. Lower limit depends on RTG background which is <10^{-7} counts/second for certain LEPT channels.

[c] Magnetic deflection separates electrons and ions for LEMPA detectors α through δ; Z measurement is single parameter.

[d] Detector δ' scans perpendicular to ecliptic plane and uses no magnetic deflection.

[e] Electrons are identified via scattering from a gold foil.

[f] All tabular data for $Z \geq 3$ are 'Nominal'. For details see Figure 8.

[g] Cosmic ray background counting rate; range extends to ~10^4 times background.

reliable and efficient from the standpoint of weight and power, and the method which
will produce the most accurate and complete data set. A gear-drive motor steps both
detector subsystems through eight positions per revolution at the rate of one
revolution per 48 minutes during the cruise mode (Figure 9). A fixed sunshield at 0°
prevents α and D1 from viewing the Sun directly (an important consideration during
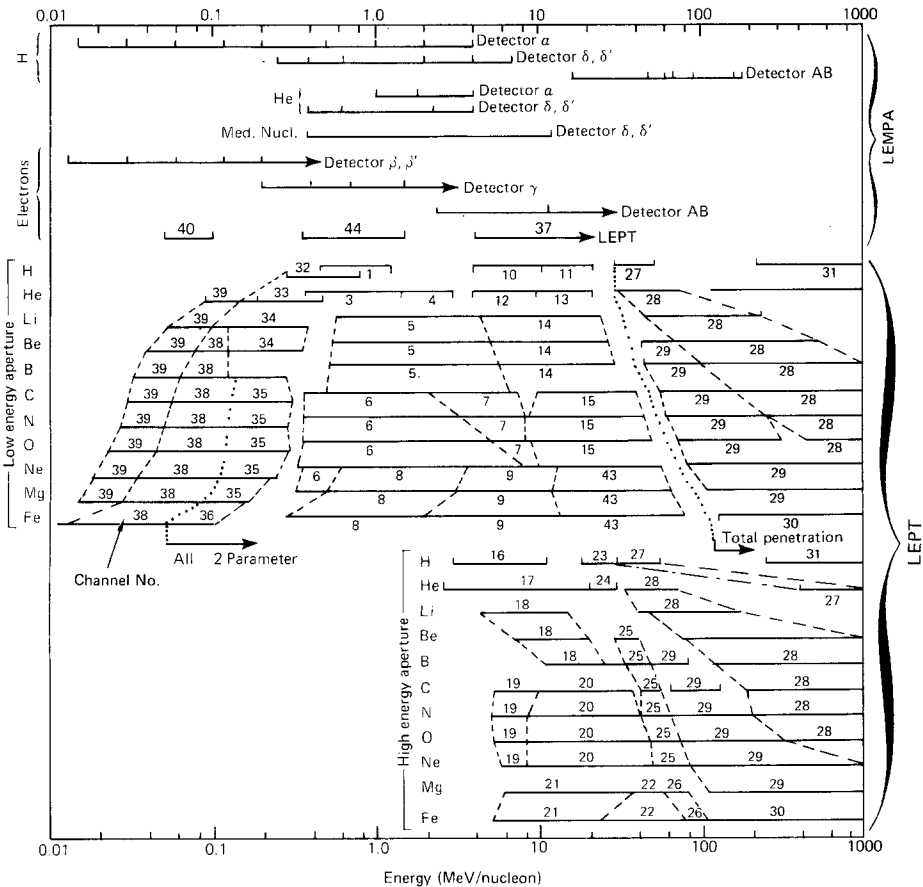the early part of the mission). During the planetary encounter mode the rate is

Fig. 8. Energy and species coverage diagram for the LECP experiment. Numbers in LEPT blocks
indicate channel number in the instrument data system. The figure is drawn for flight unit No. 1. Energy
coverage for flight unit No. 2 may differ somewhat from that shown above.

increased to one of two periods (192 sec or 48 sec), depending on availability of
spacecraft power. Normal scan sequence proceeds through sectors (Figure 9) 8-7-6-
5-4-3-2-1-1-2-3-4-5-6-7-8-8-7 .... Note that continuous rotation in one direction
is not possible because of the feed-through cable. The stepping platform can be
stopped at any position for any length of time or perform an abbreviated scan view
via ground command. Two other important applications of the stepping motor and
sunshield are: (a) it is possible to unambiguously obtain background measurements

in all detectors in all particle environments; this is particularly important in the Jovian environment where foreground from background need to be separated; (b) the sunshield contains small electron and alpha particle (Tc-99 and Am-241) radioactive sources for inflight calibrations of both subsystems.

Command and Data System (CDS)

The CDS is a major electronic subsystem of the LECP instrument which performs a large number of processing, storage, control, timing and interface functions. These functions are described very briefly below.
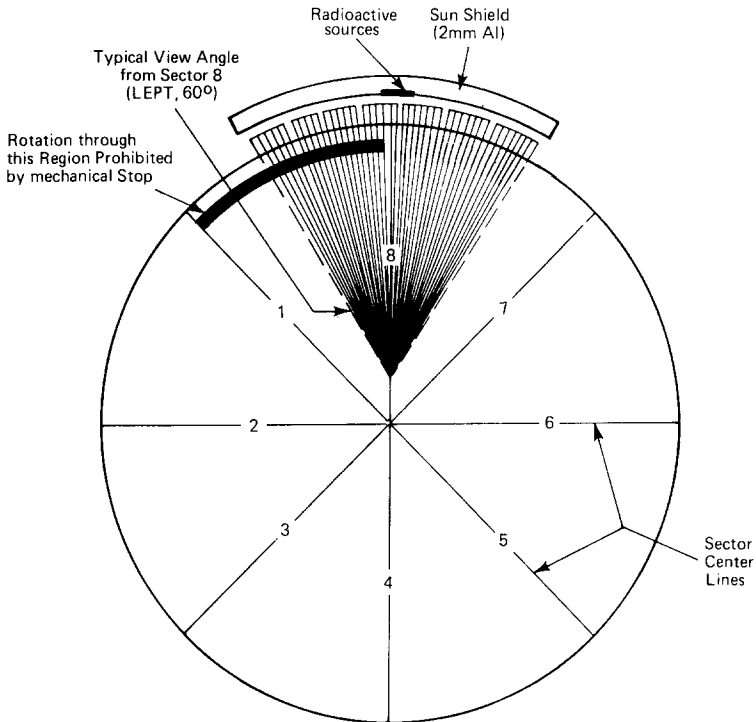
Fig. 9. Sectoring scheme for the LECP experiment detector assemblies. The sequence is 8-7-6-5-4-3-2-1-1-2-3-4-5-6-7-8-8-7- . . . . Radioactive calibration sources for both LEPT and LEMPA are mounted inside the sun shield.

The CDS accepts 42 LEPT discriminators, 33 LEMPA discriminators, and 5 coincidence strobes and generates 88 rate channels according to a set of logic equations. Rate data are accumulated in sixty-two 24-bit scalers allowing 100% duty cycle for nearly all channels. The accumulators are read in groups of four 10-bit (log-compressed) words according to one of several programs in the spacecraft Flight Data System (FDS). The rate logic is also used in the priority system to select and identify LEPT events for Pulse Height Analysis. The CDS activates the PHA system and stores four 8-bit pulse heights and an 8-bit ID code. The 40-bit PHA 'events' are

sampled by FDS command. The mode and state of the instrument are controlled by four 12-bit command words (2-bits ID, 10-bits control). The interface with the spacecraft for receipt of digital command words and for data output is fully redundant.

Modes of Operation

The measurements using the detector system described in the preceding sections are to be performed in two environments, i.e., the magnetospheres of Jupiter, Saturn and Uranus and the interplanetary medium. The magnetospheres can be further sub-divided into the distant magnetosphere (bow shock, magnetopause, tail) and near magnetosphere (trapped radiation belts). We thus utilize three modes of operation to obtain optimum science coverage:

(1) *Cruise Mode* – During this mode both detector systems will collect data, with the exception of the AB, δ and δ' subsystems of LEMPA, which are turned OFF. The stepping rate is 1 revolution in 48 minutes. This mode of operation is appropriate for the interplanetary medium where particle fluxes are not too large. The bit rate is allocated to 2/3 for the PHA data and 1/3 for the rate data.

(2) *Far Encounter Mode – Jupiter, Saturn and Uranus* – Sixty days prior to closest approach to the planet the stepping platform rate is increased to 1 revolution per minute. The experiment bit rate increases to 600 bps. At this time we allocate 1/3 of the bits to PHA data and 2/3 to rate data.

(3) *Near Encounter Mode – Jupiter* – At ~25 to $15R_J$ we will switch OFF (by command) all LEPT detectors and switch ON all remaining LEMPA detectors (i.e., AB, δ, δ').

To insure that valuable continuity in the data between LEPT and LEMPA is maintained, provisions have been made to sample each of the two subsystems on a 50% duty cycle between the Far Encounter and Near Encounter modes. This will be particularly valuable in the encounters of Saturn and Uranus, where long communication times and a totally unknown environment could compromise the measurements in any one mode.

Inflight Calibration and Housekeeping

The instruments on the Voyager mission must have an operating lifetime of at least four years, while an extended mission could increase the lifetime to perhaps ~ten years. Inflight calibrations throughout this period are therefore imperative. The calibration system for the LECP provides the following checks on instrument performance: (1) A continuous train of test pulses is fed into all preamplifier test inputs in order to maintain a check of amplifier gains, discriminator thresholds, and pulse-height analyzer linearity and performance (Peletier, 1975). (2) The test pulser determines both the 12% and 88% discriminator trigger levels so that the full-width at half-maximum noise characteristics of each pulse channel can be measured. (3) Radioactive sources mounted on the light shield provide a complete systems calibration for LEPT and LEMPA α, β, γ and δ detector systems. Thus, amplifier

gains, discriminator settings and noise readings will be read on the analog telemetry subcom; PHA linearity data will be contained in the digital data. Upon completion of the calibration sequence the LECP pulse generator will be commanded OFF.

The description of the LECP instrument in this paper has emphasized the physical description of the detectors and their applicability to various environments. A detailed description of most of the electronic subsystems is given in the paper by Peletier *et al.* (1977).

4. Summary

The experiment described here satisfies all major scientific and measurement objectives in the area of low energy charged particle investigations for both environments of interest, i.e., planetary magnetospheres and the interplanetary medium. The extremely large dynamic range ($\sim 10^{-5}$ to $> 10^{12}$ cm^{-2} sec^{-1} sr^{-1}) combined with wide coverage in energy and species assures that sufficient information will be available to characterize almost any energetic particle environment encountered by the Voyager spacecraft in a comprehensive manner. 'Second generation' studies of the Jovian magnetosphere are assured at energies, intensities, and species not available with Pioneer 10 and 11 investigations. Some of the measurements will be performed for the first time in any planetary magnetosphere (including Earth's), e.g., detailed measurements of the charge composition of trapped radiation and the full particle distribution function in three dimensions. The time resolution of the measurements (as small as ~ 60 millisec) rival those obtained in any of several Earth-orbiting spacecraft. Finally, the multiplicity of detectors coupled with built-in redundancy of key subsystems (e.g., redundant PHA's, data output lines, etc.) assures a high degree of reliability for the whole experiment.

Acknowledgements

References

Alexander, A. F. O'D.: 1965 *The Planet Uranus*, Faber and Faber, London.

Alfvén, H. and Arrhenius, G.: 1976, *Evolution of the Solar System*, NASA SP-345, 1976.

Armstrong, T. P. and Krimigis, S. M.: 1973, *Proc. 13th International Cosmic Ray Conference* **2**, 1504–1509.

Axford, W. I.: 1972 in *Solar Wind*, ed. C. P. Sonnett, P. J. Coleman, Jr. and J. M. Wilcox, NASA-SP-308, 609.

Brown, R. A.: 1973, *Proc. Copernicus Symp. IV*, IAU Symposium, No. 65, Torum, Poland.

Brown, L. W.: 1975, *Astrophys. J.* **198**, L89, 1975.

Cameron, A. G. W.: 1973, *Space Sci. Rev.* **14**, 383.

Chenette, D. L., Conlon, T. F., and Simpson, J. A.: 1974, *J. Geophys. Res.* **79**, 3551.

Dolginov, Sh. Sh., Erashenko, E. G., and Zhuzgov, L. M.: 1972, *Dokl. Akad. Nauk S.S.S.R.* **207**, 1296.

Duggal, S. P. and Pomerantz, M. A.: 1973, *J. Geophys. Res.* **78**, 7205.

Fillius, R. W. and McIlwain, C. E.: 1974, *J. Geophys. Res.* **79**, 3589.

Fisk, L. A., Kozlovsky, B., and Ramaty, R.: 1974, *Astrophys. J. (Lett.)*, **190**, L35.

Innanen, W. G. and Van Allen, J. A.: 1973, *J. Geophys. Res.* **78**, 1019.

Kennel, C. F.: 1973, *Space Sci. Rev.* **14**, 511.

Klecker, B., Hovestadt, D., Gloeckler, G., and Fan, C. Y.: 1975, *Proc. 14th International Cosmic Ray Conference*, Paper SP 2.2-8, Munich.

Krimigis, S. M., Kohl, J. W., and Armstrong, T. P.: 1975a, *Geophys. Res. Lett.* **2**, 457.

Krimigis, S. M., Sarris, E. T., and Armstrong, T. P.: 1975b, *Geophys. Res. Lett.* **2**, 561.

Mendis, D. A. and Axford, W. I.: 1974, *Annual Rev. Earth Planet. Sci.* **2**, 419.

Ness, N. F., Behannon, K. W., Lepping, R. P., and Whang, Y. C.: 1975, *J. Geophys. Res.* **80**, 2708.

Peletier, D. P., Gary, S. A., and Hogrefe, A. F.: 1977, *IEEE Trans. Nucl. Sci.*, NS-24, 795.

Peletier, D. P.: 1975, *IEEE Trans. Nucl. Sci.* NS-22, 1.

Roelof, E. C. and Krimigis, S. M.: 1973, *J. Geophys. Res.* **78**, 5375.

Roelof, E. C., Keath, E. P., Bostrom, C. O., and Williams, D. J.: 1976, *J. Geophys. Res.* **80**, 2304.

Rosenbauer, H., Grunwaldt, H., Montgomery, M. D., Paschmann, G., and Sckopke, N.: 1975. *J. Geophys. Res.* **80**, 2723.

Sarris, E. T., Krimigis, S. M., and Armstrong, T. P.: 1976, *J. Geophys. Res.* **81**, 2341.

Siscoe, G. L.: 1975, *Icarus*, **24**, 311.

Smith, E. J., Davis, L., Jr., Jones, D. E., Coleman, P. J., Jr., Colburn, D. S., Dyal, P., Sonett, C. P., and Fandsen, A. M. A.: 1974, *J. Geophys. Res.* **79**, 3501.

Smith, E. J. and Wolfe, J. H.: 1976, *Geophys. Res. Lett.* **3**, 137.

Thomsen, M. F. and Van Allen, J. A.: 1976, *Astrophys. J.* **206**, 599.

Teegarden, B. J., McDonald, F. B., Trainor, J. H., Webber, W. R., and Roelof, E. C.: 1974, *J. Geophys. Res.* **79**, 3615.

Wibberenz, G., Lanzerotti, L. J., and Venkatesan, D.: 1976, *J. Geophys. Res.* **81**, 5807.

Williams, D. J.: 1975 in V. Formisano (ed.), *The Magnetospheres of Earth and Jupiter*, D. Reidel, Dordrecht, Holland, p. 161.

Williams, D. J. and Lyons, L. R.: 1974, *J. Geophys. Res.* **79**, 4195.

Wolfe, J. H., Mihalov, J. D., Collard, H. R., McKibbin, D. D., Frank, L. A., and Intriligator, D. S.: 1974, *J. Geophys. Res.* **79**, 3489.